Three dimensional modeling of the galactic cosmic ray intensity variation with the changeable solar wind velocity

M.V. Alania, R Modzelewska, A. Wawrzynczak

***Abstract*— We develop a three dimensional (3-D) models of the 27-day variation and Forbush decrease (Fd) of galactic cosmic ray (GCR) intensity taking into account the changeable solar wind velocity. The proposed models are justified by the solution of the equation $div\, B = 0$ of the Interplanetary Magnetic field (IMF) B for the azimuthally dependence of the radial component of the solar wind velocity. We show that the proposed models are more realistic and compatible with the experimental data.**

1. Introduction

To investigate various type of the galactic cosmic rays (GCR) intensity variations (e.g. 27-day, Forbush decreases) spatial and time dependences of the solar wind velocity V and the interplanetary magnetic field (IMF) B should be taken into account. In this case there is necessary to solve a system of equations keeping validness of the $div\, B = 0$. Maxwell's equations for the IMF strength B have a form [1]:

$$\begin{cases} \dfrac{\partial B}{\partial t} = \nabla \times (V \times B) & (1a) \\ div\, B = 0 & (1b) \end{cases}$$

where, B is strength of the IMF, V –solar wind velocity, and t -time. For the components B_r, B_θ, and B_φ of the IMF and components $(V_r, V_\theta, V_\varphi)$ of the solar wind velocity the system of equations (1a)-(1b) for the stationary case $\left(\dfrac{\partial B}{\partial t} = 0\right)$ in the heliocentric spherical (r, θ, φ) coordinate system can be rewritten, as:

$$\begin{cases} \dfrac{1}{r^2 \sin\theta}\left[\dfrac{\partial}{\partial \theta}[(V_r B_\theta - V_\theta B_r) r \sin\theta] - \dfrac{\partial}{\partial \varphi}[(V_\varphi B_r - V_r B_\varphi) r]\right] = 0 & (2a) \\ \dfrac{1}{r \sin\theta}\left[\dfrac{\partial}{\partial \varphi}(V_\theta B_\varphi - V_\varphi B_\theta) - \dfrac{\partial}{\partial r}[(V_r B_\theta - V_\theta B_r) r \sin\theta]\right] = 0 & (2b) \\ \dfrac{1}{r}\left[\dfrac{\partial}{\partial r}[(V_\varphi B_r - V_r B_\varphi) r] - \dfrac{\partial}{\partial \theta}(V_\theta B_\varphi - V_\varphi B_\theta)\right] = 0 & (2c) \\ \dfrac{1}{r^2}\dfrac{\partial}{\partial r}(r^2 B_r) + \dfrac{1}{r \sin\theta}\dfrac{\partial}{\partial \theta}(\sin\theta B_\theta) + \dfrac{1}{r\sin\theta}\dfrac{\partial}{\partial \varphi} B_\varphi = 0 & (2d) \end{cases}$$

The system of equations (2a)-(2d) is rather complicated and it can be solved only by the numerical method.

M. V. Alania Institute of Math. And Physics of University of Podlasie, Siedlce, Poland; Institute of Geophysics, Georgian Academy of Sciences, Tbilisi, Georgia (e-mail: alania@ap.siedlce.pl).

R. Modzelewska, Institute of Math. And Physics of University of Podlasie, Siedlce, Poland (e-mail: renatam@ap.siedlce.pl).

A. Wawrzynczak, Institute of Computer Science of University of Podlasie, Siedlce, Poland (e-mail: awawrzynczak@ap.siedlce.pl).

We consider that an average value of the heliolatitudinal component of the solar wind velocity V_θ equals zero $(V_\theta \approx 0)$, and the equations (2a)-(2d) can be reduced to the form:

$$\begin{cases} r\sin\theta\, V_r \dfrac{\partial B_\theta}{\partial \theta} + r\sin\theta B_\theta \dfrac{\partial V_r}{\partial \theta} + r\cos\theta\, V_r B_\theta - rV_\varphi \dfrac{\partial B_r}{\partial \varphi} - rB_r \dfrac{\partial V_\varphi}{\partial \varphi} + r\, V_r \dfrac{\partial B_\varphi}{\partial \varphi} + rB_\varphi \dfrac{\partial V_r}{\partial \varphi} = 0 & (3a) \\ V_\varphi \dfrac{\partial B_\theta}{\partial \varphi} + B_\theta \dfrac{\partial V_\varphi}{\partial \varphi} + r\sin\theta\, V_r \dfrac{\partial B_\theta}{\partial r} + r\sin\theta\, B_\theta \dfrac{\partial V_r}{\partial r} + \sin\theta\, V_r B_\theta = 0 & (3b) \\ rB_r \dfrac{\partial V_\varphi}{\partial r} + rV_\varphi \dfrac{\partial B_r}{\partial r} + V_\varphi B_r - V_r B_\varphi - rV_r \dfrac{\partial B_\varphi}{\partial r} - rB_\varphi \dfrac{\partial V_r}{\partial r} + B_\theta \dfrac{\partial V_\varphi}{\partial \theta} + V_\varphi \dfrac{\partial B_\theta}{\partial \theta} = 0 & (3c) \\ \dfrac{\partial B_r}{\partial r} + \dfrac{2}{r} B_r + \dfrac{ctg\,\theta}{r} B_\theta + \dfrac{1}{r}\dfrac{\partial B_\theta}{\partial \theta} + \dfrac{1}{r\sin\theta}\dfrac{\partial B_\varphi}{\partial \varphi} = 0 & (3d) \end{cases}$$

In this paper our aim is to build up models of the 27-day variation and Forbush decrease (Fd) of the GCR intensity using only two dimensional IMF. So, there is possible to make certain simplification of the system of equations (2a)-(2d). We assume that latitudinal component B_θ of the IMF equals zero $(B_\theta = 0)$; this assumption straightforwardly leads (from (3a)) to the relationship between B_r and B_φ, as, $B_\varphi = -B_r \frac{V_\varphi}{V_r}$. Then (3d) with respect to the radial component B_r has a form:

$$A_1 \frac{\partial B_r}{\partial r} + A_2 \frac{\partial B_r}{\partial \varphi} + A_3 B_r = 0 \qquad (4)$$

Coefficients A_1, A_2 and A_3 depend on the radial V_r and heliolongitudinal V_φ components of the solar wind velocity V.

2. Experimental data and Model of the 27-day variation of the GCR intensity

In recent papers [2]-[5] was shown that the heliolongitudinal asymmetry of the radial component of the solar wind (SW) velocity is one of important source of the 27-day variation of the GCR intensity and anisotropy. Regarding the simultaneous enhancements of the quasi periodic changes of the GCR intensity and parameters of solar wind was mentioned in paper [6] for the positive polarity periods of the solar activity minimum epochs.

In this paper we analyze daily experimental data of the solar wind velocity (upper panel of Fig. 1), GCR intensity from Moscow neutron monitor (middle panel of Fig. 1) and IMF (bottom panel of Fig. 1) for the period of August 2007-February 2008.

There are clear changes of the 27-day variations of the solar wind velocity and the GCR intensity being in opposite phase. Besides, the dominated 27-days and relatively weaker 14 days waves in the solar wind velocity changes there is observed also a clear third harmonic (~9 days). Generally higher harmonics in the solar rotation period (e.g. 14 and 9 days) are related with the simultaneous existence of several active heliolongitudes [7]. Recently, by [8] were provided strong evidence that the 9-day period in the solar wind parameters might be caused by the periodic longitudinal distribution of coronal holes on the Sun recurring for several Carrington rotations.

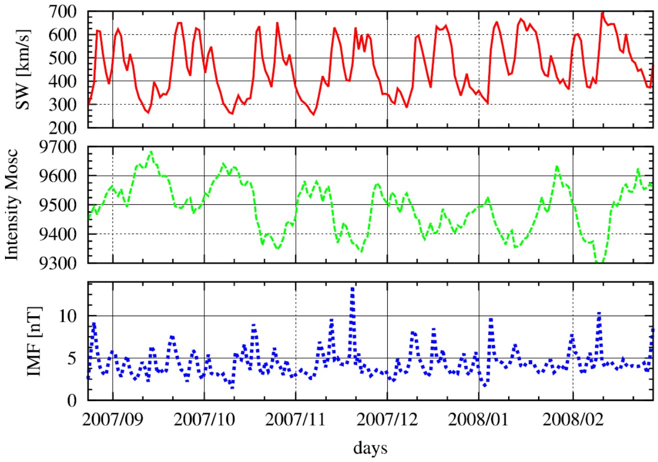

Fig. 1 Temporal changes of the daily solar wind velocity (SW) [OMNI], GCR intensity for Moscow neutron monitor and IMF [OMNI] for the period of 24 August 2007-28 February 2008

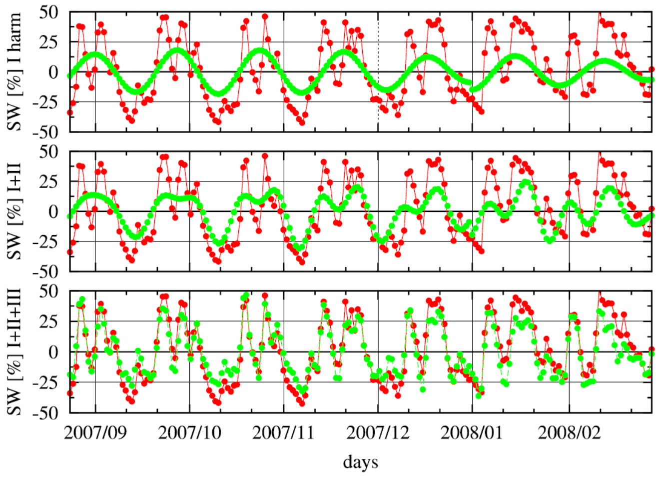

Fig. 2 Temporal changes of the daily solar wind velocity with the fitting by a 27-day (I harmonic), 14-day (II harmonic) and 9-day (III harmonic) wave for the period of 24 August 2007-28 February 2008

In Fig. 2 are presented temporal changes of the observed solar wind velocity and first (27 days) harmonic (upper panel), sum of the first (27 days) and second (14 days) harmonics (middle panel), and sum of the first (27 days), second (14 days), and third (9 days) harmonics (bottom panel). It is seen that there is an apparent fitness between the sum of three (27, 14 and 9 days) harmonics and the experimental data of the solar wind velocity.

In Fig. 3 are presented temporal changes of superimposed SW velocity data (points) with theirs fitting (dashed line) by the sum of first three (27, 14 and 9 days) harmonics for the period of August 2007- February 2008.

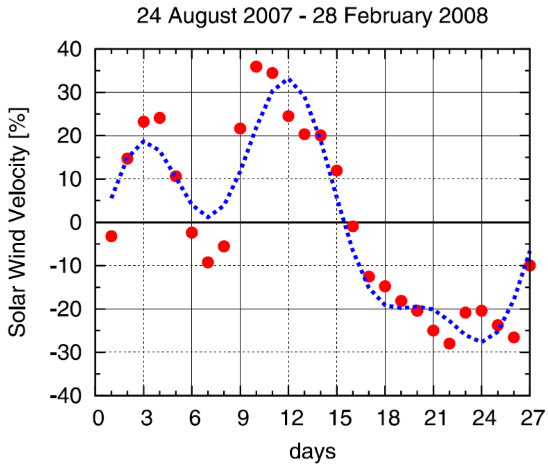

Fig. 3 Temporal changes of superimposed SW velocity data (points) with theirs fitting (dashed line) by a sum of first three (27, 14 and 9 days) harmonics for the period of 24 August 2007-28 February 2008

2.1. *Numerical solution for the IMF*

Our goal is to solve the equation (4) in heliocentric coordinate system (r,θ,φ) for the changeable solar wind velocity as much as possible corresponding to the in situ measurements in the interplanetary space. So, we include in (4) the expression approximating the changes of the average radial solar wind velocity calculated based on the experimental data (dashed line in Fig. 3):

$$V_r = 400\times(1+\alpha_1\sin(\varphi-0.5)+\alpha_2\sin(2(\varphi-0.9))+\alpha_3\sin(3(\varphi-0.15))) \quad (5)$$

where, φ is heliolongitude $\alpha_1 = 0.2275 \quad \alpha_2 = -0.0925 \quad \alpha_3 = 0.106$

We take into account, as well:

$$V_\theta = 0, \quad V_\varphi = \Omega r\sin\theta \quad (6)$$

Taking into consideration the expressions (5) and (6) the coefficients A_1, A_2 and A_3 in (4) have the form:

$$A_1 = 1$$

$$A_2 = -\frac{\Omega}{400\times(1+\alpha_1\sin(\varphi-0.5)+\alpha_2\sin(2(\varphi-0.9))+\alpha_3\sin(3(\varphi-0.15)))}$$

$$A_3 = \frac{2}{r} + \frac{400\times\Omega\times(\alpha_1\cos(\varphi-0.5)+2\alpha_2\cos(2(\varphi-0.9))+3\alpha_3\cos(3(\varphi-0.15)))}{(400\times(1+\alpha_1\sin(\varphi-0.5)+\alpha_2\sin(2(\varphi-0.9))+\alpha_3\sin(3(\varphi-0.15))))^2}$$

Equation (4) can be solved only numerically, and for this purpose we use a difference scheme method e. g., [9].

Equation (4) does not contain derivative with respect the heliolatitude θ, but there is an implicit dependence of the B_r on the θ through coefficients A_1, A_2 and A_3, i.e., θ plays role of the parameter. In this case we have a possibility of the methodical choice, either construct three dimensional (3-D) difference scheme consider B_r as a function of the heliocentric coordinates (r,θ,φ), and then solve (4) for any possible changes of θ, or construct (2-D) difference scheme consider B_r as a function of the heliocentric coordinates r and φ, and solve (4) for any possible changes of the parameter θ. In this paper we use the first method. Equation (4) was reduced to the algebraic system of equations using a difference scheme method e. g., [9], as:

$$A_1 \frac{B_r[i+1,j,k]-B_r[i,j,k]}{\Delta r}+A_2\frac{B_r[i,j,k+1]-B_r[i,j,k]}{\Delta\varphi}+A_3B_r[i,j,k]=0 \qquad (7)$$

where, i=1,2,…, I; j=1,2,…,J; k=1,2,…, K (I = 107 – is number of steps in radial distance, J =79 - vs. heliolatitude, and K=36, vs. heliolongitude). Then (7) was solved by the iteration method with the boundary condition near the Sun $B_r[1,j,k]=const$; in considered case r_1 =0.5 AU, $B_r[1,j,k]=25\,nT \quad for \quad 0^0\le\theta\le 90^0 \quad and \quad -25\,nT \quad for \quad 90^0<\theta\le 180^0$ for the positive polarity period (A>0).

The choice of these boundary conditions was stipulated by the demanding of the coincidence of the solutions (7) with the in situ measurements of the B_r and B_φ components of the IMF.

Results of the solution of (7) for the B_r and B_φ calculated by the expression $B_\varphi=-B_r\frac{V_\varphi}{V_r}$ are presented in Figs. 4-5, respectively.

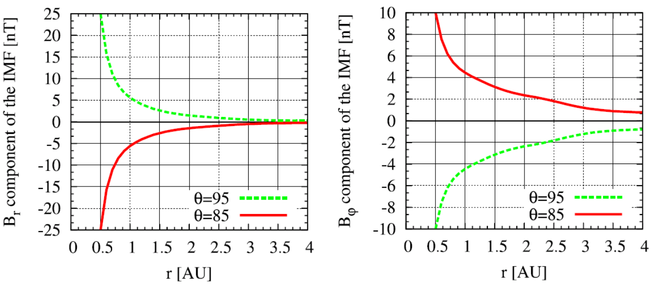

(a) (b)

Fig. 4ab Radial changes of the (a) B_r and (b) B_φ components of the IMF for different heliolatitudes near the solar equatorial plane

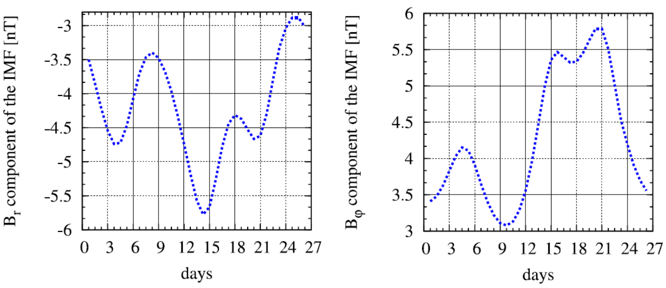

(a) (b)

Fig. 5ab Azimuthal changes of the (a) B_r and (b) B_φ components of the IMF at the Earth orbit

In Figs. 5cd are presented heliolatitudinal changes of the B_φ component of the IMF at 1 AU, found by the expression $B_\varphi=-B_r\frac{V_\varphi}{V_r}$, and azimuthal changes of the magnitude $B=\sqrt{B_r^2+B_\varphi^2}$ of the IMF at the Earth orbit, respectively.

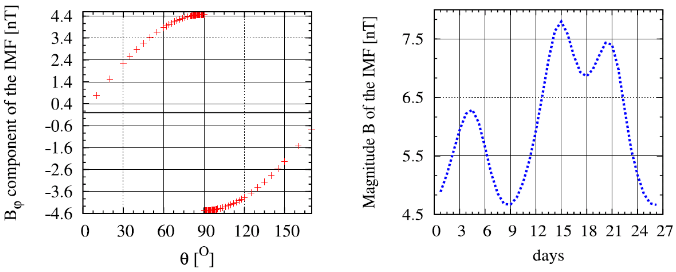

(c) (d)

Fig. 5 (c) Heliolatitudinal changes of the B_φ component of the IMF at 1 AU; (d) azimuthal changes of the magnitude B of the IMF at the Earth orbit

2.2 Modeling of the 27-day variation of the GCR intensity

For the modeling of the 27-day variation of the GCR intensity we use Parker's transport equation [10]

$$\frac{\partial N}{\partial t}=\nabla_i\left(K_{ij}\nabla_j N\right)-\nabla_i\left(V_i N\right)+\frac{1}{3}\frac{\partial}{\partial R}\left(N R\right)\nabla_i V_i \qquad (8)$$

Where N and R are density and rigidity of cosmic ray particles, respectively; V_i – solar wind velocity, t is time, K_{ij} is the anisotropic diffusion tensor of galactic cosmic rays.

We consider a stationary case, $\frac{\partial N}{\partial t}=0$. In equation (8) were included B_r and B_φ components of the IMF obtained based on the numerical solution of (7), and the changes of the radial solar wind velocity (5), as well. To exclude an intersection of the IMF lines the heliolongitudinal asymmetry of the SW velocity takes place only up to the distance of ~ 8 AU and then $V=400\,km/s$ throughout the heliosphere. In connection with this behind 8 AU in the theoretical model standard Parker's field is used. Equation (8) was solved numerically as presented in our papers published elsewhere [2], [4].

Results of calculations of the 27-day variation of the GCR intensity based on the solution of (8) are presented in Fig. 6 (dashed line); in this figure are presented (points) changes of the GCR intensity obtained for Moscow neutron monitor experimental data averaged for 7 Carrington rotations during the period of 24 August 2007-28 February 2008 (middle panel of Fig. 1), as well.

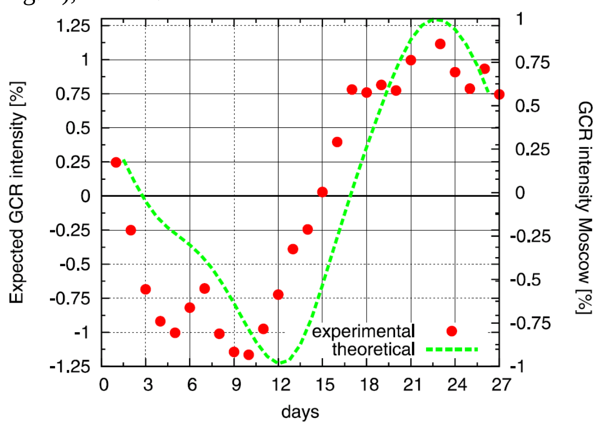

Fig. 6 Heliolongitudinal changes of the expected GCR intensity for rigidity 10GV at the Earth orbit during solar rotation period (dashed line) in comparison with temporal changes of superimposed Moscow GCR intensity data during 27 day for the period of 24 August 2007-28 February 2008 (points)

Fig. 6 shows that results of theoretical modeling (dashed line) and the experimental data (points) are in good agreement. We conclude that the presented model of the 27-day variation of the GCR intensity composed using the changeable solar wind velocity (5) and values of the components B_r and B_φ obtained as the solutions of (7) is good enough compatible with the experimental data.

3. Experimental data and Model of the reccurrent Forbush decrease

3.1 Experimental data

We analyze daily changes of the experimental data of the IMF (upper panel of Fig. 7), GCR intensity from Moscow neutron monitor (middle panel of Fig. 7) and the solar wind velocity (bottom panel of Fig. 7) for the period of 6-20 August 1994. Changes of the GCR intensity for the period of 6-20 August 1994 (to the first approximation) can be considered as a recurrent Fd.

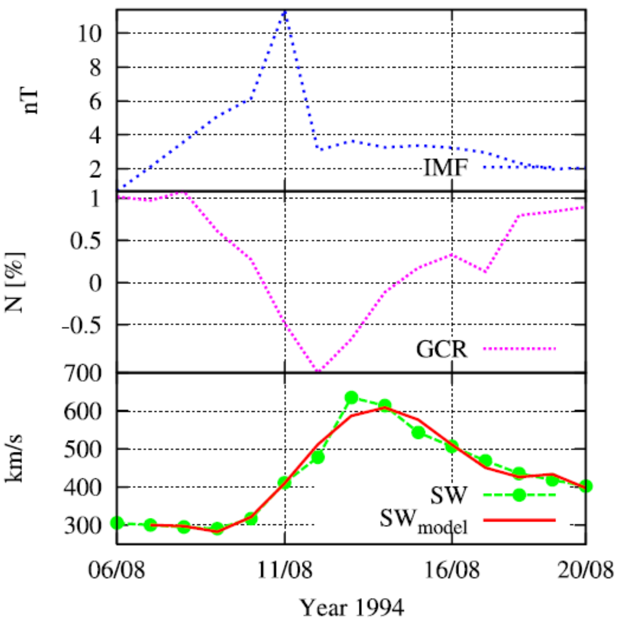

Fig. 7. Daily data of IMF (OMNI) (top panel), GCR intensity (Moscow NM) (middle panel) and solar wind velocity (dotted panel, solid observed by SOHO, dotted considered in the model of the Fd) in period of 6-20 August 1994. Changes of GCR intensity in periods of 6-20 August 1994 can be considered as a recurrent Fd.

3.2 Modeling of the Forbush decrease of the GCR intensity

To compose the model of the Fd we found the solution of (7) for the solar wind velocity as much as possible corresponding to the experimental data of the period 6-20 August 1994 (Fig. 7) and presented, as:

$$V_r = 300 * \begin{pmatrix} -0.1857\varphi^6 + 3.3538\varphi^5 - 24.273\varphi^4 \\ +89.574\varphi^3 - 176.94\varphi^2 + 177.41\varphi \\ -69.755 \end{pmatrix} * (\sin(\theta) + 0.2)) \quad (9)$$

In Fig. 7 dotted line corresponds to the expression (9) describing the changes of the assumed solar wind velocity, and dashed line – to the experimental data (bottom panel of Fig. 7). The components B_r and B_φ obtained as the solutions of (7) for the changes of the solar wind velocity of type (9) are presented in Figs. 8 and 9.

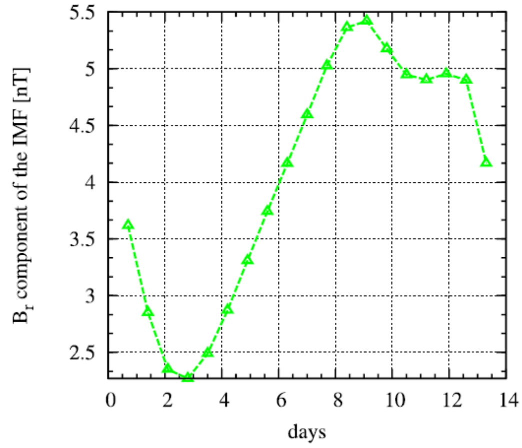

Fig. 8. Azimuthal changes of the B_r component of the IMF at the Earth orbit during the Fd.

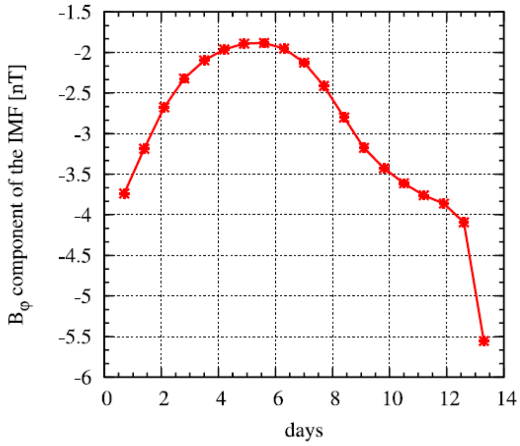

Fig. 9. Azimuthal changes of the B_φ component of the IMF at the Earth orbit during the Fd.

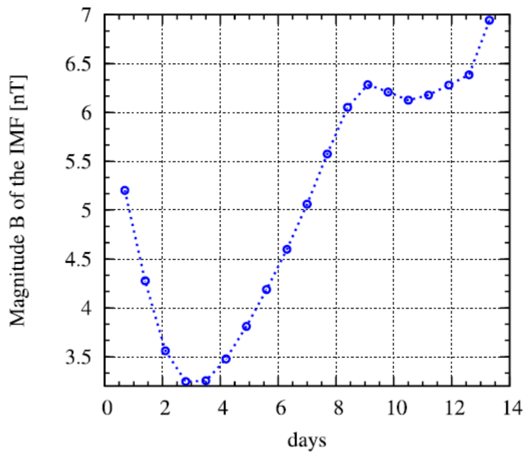

Fig. 10. Azimuthal changes of the magnitude B of the IMF at the Earth orbit during the Fd.

To construct the model of the Fd of the GCR intensity we use Parker's transport equation (8) including the B_r and B_φ components and magnitude B (Figs. 8-10) of the IMF obtained based on the solutions of (7) and solar wind velocity changes according to (9) corresponding to the experimental data (bottom panel of Fig. 7). Also, we assume that in the formation of the Fd of the GCR intensity an important role belongs to the changes of the diffusion coefficient K_{II} caused by the changes of the IMF turbulence [11]-[13]. In the proposed model a diffusion coefficient K_{II} is presented as: $K_{II} = K_0\, K(r)\, K(R,r,\varphi)$, were $K_0 = 4.5\times10^{21}\ cm^2/s$, $K(r) = 1 + 0.5\left(\frac{r}{1AU}\right)$; here r is heliocentric distance, φ - heliolongitude. The decrease of diffusion coefficient K_{II} is caused by the increase of the IMF turbulence e.g. [11]-[13]. The change of the IMF turbulence in the energy range of frequency (10^{-6}- 10^{-5} Hz) is reflected in the increasing of the exponent ν of the power spectral density (PSD) of the IMF ($PSD \propto f^{-\nu}$). We suppose that the exponent ν increases in the vicinity of space responsible for the Fd as: $\nu(\varphi) = 0.8 + 0.1*(\cos(\varphi) - 0.2)$ causing the decrease of the diffusion coefficient due to dependence $K(R,\varphi) = R^{\alpha'(\varphi)} = R^{2-\nu(\varphi)}$, [14]-[16].

In Fig. 11 are presented the changes of the diffusion coefficient (squares line) and the solar wind velocity (triangles line) at the Earth orbit included in the model of the Fd.

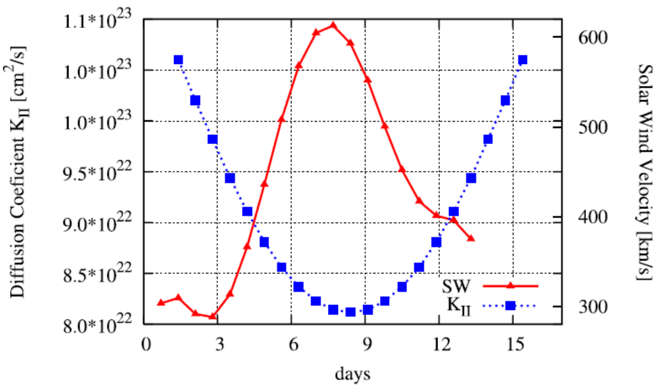

Fig 11. Changes of the diffusion coefficient and the solar wind velocity at the Earth orbit included in the model of the Fd.

Equation (8) was solved numerically as presented in our papers published elsewhere e.g. [12], [13]. Changes of the relative density obtained as a solution of the transport equation for the model of the Fd are presented in Fig. 12. One can see that the obtained results are compatible with the experimental observations e.g. in period of 6-20 August 1994 (Fig.7).

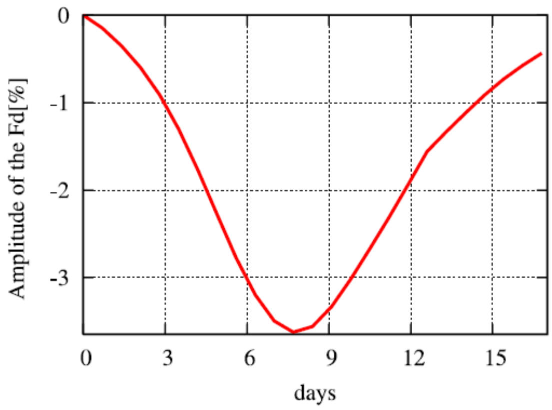

Fig 12 Changes of the expected amplitude of the Fd of the GCR intensity for the rigidity of 10 GV based on the solution of the model of the Fd with changeable solar wind velocity

4. CONCLUSIONS

1. Three dimensional models of the 27-day variation and recurrent Fd of the GCR intensity are proposed including the spatial changeable solar wind velocity, and B_r and B_φ components of the IMF obtained as the numerical solutions of the Maxwell's equations.
2. Proposed model of the 27-day variation of GCR intensity is compatible with the experimental data of GCR intensity.
3. The proposed model of the recurrent Fd well represents processes which take place in the interplanetary space during the Fd, i.e. the increase of the IMF turbulence and the increase of the solar wind velocity.
4. Creation of the models of GCR modulation with the spatial changeable solar wind velocity, and corresponding B_r and B_φ components of the IMF (obtained as the numerical solutions of the Maxwell's equations) gives a possibility to build more realistic models for various classes of GCR modulation. Possibilities to construct more realistic but rather complicated models of different classes of GCR variations can be extended based on the solutions of Maxwell's equations for three dimensional case.

ACKNOWLEDGMENTS

Authors thank the investigators of neutron monitors stations, SOHO and Advanced Composition Explorer spacecrafts for possibility to use their data.

REFERENCES

[1] E. N. Parker, "Interplanetary Dynamical Processes", *Interscience Publishers*, New York, 1963

[2] A. Gil, M. V. Alania, "27-day variation of cosmic rays for the minima epochs of solar activity: experimental and 3-D drift modeling results", *Proc. 27th ICRC*, Hamburg, 9, 2001, pp. 3725-3728

[3] E. S. Vernova, M. I. Tyasto, D. G. Baranov, M. V. Alania, A. Gil, "On the influence of solar activity and the solar magnetic field on the 27-day variation of galactic cosmic rays", *Adv. Space Res.*, 32, 4, 2003, pp. 621-626

[4] R. Modzelewska M.V. Alania, A. Gil, K. Iskra, "27-day variations of the galactic cosmic ray intensity and anisotropy", *Acta Phys. Pol. B* 37, 5, 2006, pp. 1641-1650

[5] M. V. Alania, A. Gil, R. Modzelewska, „Study of the 27-day variations of the galactic cosmic ray intensity and anisotropy", *Adv. Space Res*. 41, 1, doi:10.1016/j.asr.2007.06.001, 2008, pp. 280 – 286

[6] I. G. Richardson, H. V. Cane, G. A. Wibberenz, "A 22-year dependence in the size of near-ecliptic corotating cosmic ray depressions during five solar minima", *J. Geophys. Res*. 104, 1999, pp. 12549–12553

[7] M. V. Alania, L. Kh. Shatashvili, "Quasi-periodic Cosmic Ray variations", Mecniereba, Tbilisi, 1974 (In Russian)

[8] M. Temmer, B. Vršnak, A. M. Veronig, "Periodic Appearance of Coronal Holes and the Related Variation of Solar Wind Parameters", *Solar Phys*., 241, 2, 2007, pp. 371-383

[9] D. Kincaid, W. Cheney, "Numerical Analysis", WNT, Warsaw, 2006

[10] E. N. Parker, "The passage of energetic charged particles through interplanetary space", *Planet. and Space Sci.*, 13, 1965, pp. 9-49

[11] A. Wawrzynczak, M. V. Alania, "Peculiarities of galactic cosmic ray Forbush effects during October-November 2003", *Adv. Space Res*., 35, 2005, pp. 682-686

[12] A. Wawrzynczak, M. V. Alania, "Modeling of the recurrent Forbush effect of the galactic cosmic ray intensity and comparison with the experimental data", *Adv Space Res*.,41, 2, 2008, pp. 325-334

[13] Alania, M.V., Wawrzynczak, A., „Forbush decrease of the Galactic Cosmic Ray Intensity:Experimental Study and Theoretical Modeling" *Astrophys. And Space Sci. Transactions*, 2008 , to be published

[14] Hasselman, K. and Wibberentz, G.: Scattering of charged particles by random electromagnetic field, *Z. Gephys*., 34, 353, 1968.

[15] J. R. Jokipii, "Propagation of Cosmic rays in The Solar Wind", *Reviews of Geophysics and Space Physics*, 9,1, 1971, pp. 27-87

[16] I. N. Toptygin, "Cosmic rays in interplanetary magnetic fields", *Reidel Publishing Company*, 1985